ELSEVIER

Biophysical Chemistry 75 (1998) 201–211

Biophysical Chemistry

Diffusion of transferrin receptor clusters

Mamta Srivastava, Nils O. Petersen*

Department of Chemistry, The University of Western Ontario, London, Ontario, Canada N6A 5B7

Received 14 July 1998; received in revised form 21 September 1998; accepted 22 September 1998

Abstract

Two dimensional motion of membrane receptors provides a mechanism for interaction among receptors in the plane of the membrane. In some cases the lateral diffusion leads to formation of clusters which may also be mobile. We have used image cross-correlation (ICCS) spectroscopy technique to measure the translational motion of transferrin receptors in the membrane of 3T3 fibroblasts and HEp2 carcinoma cells. The technique is based on the measurement and analysis of fluctuations in the intensity observed in fluorescence confocal microscope images measured as a function of time. The fluorescence fluctuations arise from stochastic concentration fluctuations about the equilibrium concentration caused by movement of receptors. The amplitude of the fluctuations depend on the number of fluorescent molecules in the observation volume and the dynamics provide the rate of movement. The diffusion observed by this analysis is orders of magnitude slower than that measured by conventional photobleaching techniques. The slower motion corresponds to the diffusion of receptor clusters which provide the more dominant fluctuations.

Keywords: Cross-correlation; Confocal scanning laser microscopy; ICCS; Membrane dynamics; Photobleaching; Transferrin receptors

1. Introduction

Uptake of nutrients by cells is often mediated by receptors on the cell surface. For example, transferrin, an iron carrier, binds to a transferrin receptor which is then localised to coated pits. These invaginate to form coated vesicles carrying the receptors and the transferrin inside for further processing. The initial part of the uptake depends on the ability of the receptors to move laterally in the membrane to find a coated pit. We are interested in understanding the dynamics of the interactions of transferrin receptors with the coated pit and have developed methods to investigate these quantitatively. One question of interest is whether transferrin clusters (in coated pits) are

* Corresponding author.

0301-4622/98/$ - see front matter
PII S0301-4622(98)00206-3

also mobile. Measurement of the lateral mobility of membrane proteins, such as receptors, is helpful for understanding the dynamics of cell surface processes [1,2]. Consequently several elegant techniques, most of which rely on fluorescence microscopy, have been developed to characterize the diffusion of lipids and proteins on the surface of living cells [3–28]. These have shown that membrane proteins and lipids diffuse laterally in the membrane plane unless constrained by interactions with immobile or slowly moving components.

Since the development of the fluorescence photobleaching methods, the lateral mobility of membrane constituents has been probed extensively [6,29–33] assuming free Brownian diffusion of cell surface receptors in two dimensions. The very extensive application of this and related techniques has clearly demonstrated that lateral mobility of most proteins in cell membrane is highly restricted. Single particle tracking experiments [19,20,25,26,28,34,35] indicate that while some receptors undergo random diffusion, others undergo diffusion restricted to domains [18]. Diffusion coefficients are generally several orders of magnitude less than those measured for proteins diffusing freely in reconstituted bilayer membranes and even immobile components are also observed.

Here we describe a fluorescence technique: image cross-correlation spectroscopy (ICCS) [36] designed to measure mobility (diffusion) of receptor clusters (aggregates) on cell surfaces. The technique is based on accumulating a series of confocal microscopy images at a fixed interval of time. A cross-correlation function is calculated by correlating the image collected at one time with the image collected at a later time. The amplitude of the cross-correlation function will reveal the average persistence of fluctuations at all the positions in the image during the delay. Analysis of the rate and shape of the temporal decay of the amplitude of the cross-correlation functions obtained this way provides information about the dynamic processes that give rise to fluorescence fluctuations from image to image. This report is intended to illustrate the application of the ICCS technique to measurement of the lateral diffusion of transferrin receptor clusters on the surface of live 3T3 fibroblasts and HEp2 (human epidermoid carcinoma) cells. We compare these results to diffusion measurements of transferrin receptors using fluorescence photobleaching.

2. Materials and methods

2.1. Labelling for diffusion measurements

Mouse 3T3 fibroblasts and human HEp2 cells were obtained from American Type Culture Collection (ATCC), Rockville, MD, USA. Mouse 3T3 fibroblasts were grown in Dulbecco's Modified Eagle's Medium (DMEM) containing L-glutamine (2 mM) and 10% fetal bovine serum and supplemented with penicillin (50 U/ml) and streptomycin (50 μg/ml). HEp2 cells were grown in Minimum Essential Medium (MEM) also containing L-glutamine and 5% fetal bovine serum and penicillin (100 U/ml) and streptomycin (100 μg/ml). The cell lines were cultured at 37°C in a humidified incubator with 5% CO_2. For microscopy experiments trypsinised cells were seeded on 18-mm-diameter glass coverslips placed in tissue culture petri dishes in the same medium. 3T3 fibroblasts were used for experiments on the third day of subculture and HEp2 cells were used on the second day of subculture. All samples were treated at 4°C (on ice) to inhibit internalization of labelled receptors. Cells were washed twice with cold PBS^+ (PBS with $CaCl_2$ and $MgCl_2$) then incubated for 30 min with the primary antibody (FITC labelled monoclonal anti-mouse transferrin receptors) in the case of 3T3 cells and (FITC labelled monoclonal anti-human transferrin receptors) in the case of HEp2 cells. Cells were washed again twice for 5 min with cold PBS^+ and mounted on coverslips with the cells upside down onto microscope slides using a 'mounting medium'. Antibody solutions were diluted in PBS^- (PBS without $CaCl_2$ and $MgCl_2$). The mounting medium was prepared by mixing 20 g Airvol (203) in 80 g water and stirring the mixture vigorously while warming it to 60–70°C for 1–2 h followed by adding 40 ml of a glycerol/*n*-propyl gallate (0.2 g) solution and 0.2 ml of a 0.2 M tris buffer (pH 8.5). The solution is centrifuged at

more than $18\,000 \times g$ to remove particles. The prepared mounting medium is stored at -20°C in small aliquots.

2.2. Labelling for distribution measurements

To measure the distribution of transferrin receptors on the cell surface cells were washed twice with cold PBS^+ then fixed in a 4% cold paraformaldehyde solution in PBS^+ for 15 min. Paraformaldehyde fixation was conducted in order to stop diffusion of membrane receptors. Cell fixation hinders the function and mobility of the cell surface components by chemically crosslinking them. We have shown previously that paraformaldehyde fixation essentially freezes the cell surface [37]. Moreover paraformaldehyde treatment does not appreciably change receptor labelling as demonstrated by electron microscopy studies [38,39]. After washing with 5 ml PBS^+, cells were soaked twice with 0.1 M glycine in PBS^+ for 5 min at room temperature. Following washing twice with 5 ml PBS^+ and twice with PBS^+ with 1% BSA, the cells were incubated for 30 min with the primary antibody (FITC labelled monoclonal anti-mouse transferrin receptors in case of 3T3 cells and FITC labelled monoclonal anti-human transferrin receptors in case of HEp2 cells). Cells were then washed twice for 5 min with PBS^+ to remove non-specifically bound antibody and mounted on coverslips with the cells upside down onto microscope slides using the mounting medium. A number of confocal images were measured on sections of the cells. Care was taken to avoid any edges of the cells and areas on or near the nucleus in order to obtain a nice flat area of the cell.

2.3. Confocal microscopy

Confocal microscopy was performed at room temperature (25 ± 2°C) on a Biorad MRC-600 laser scanning confocal microscope equipped with a Nikon inverted microscope to obtain two dimensional fluorescence images of areas on the cell membrane. Calibration procedure for the photon counting mode was followed as outlined in the Biorad MRC 600 user's manual. The gain and black levels were set to prevent saturation and to ensure a low but non-zero background. The black level was set high enough so that photons were detected in every pixel. Samples were examined through a $60\times$, 1.4NA oil immersion objective using a 25 mW argon ion laser at 488 nm as the illumination source. The fluorescence was detected by the photomultiplier tube operating in the analogue mode for the FITC labelled samples. Filter combinations appropriate for fluorescein (excitation filter 488 DF 10, dichroic reflector 510 LP, emission filter OG 515 LP) were used in an epifluorescence mode. The pinhole aperture was opened to setting 10 on the Biorad vernier scale corresponding to 5.8 mm diameter. This is in contrast to the optical sectioning experiments normally performed using confocal microscope. The confocal pinhole in the confocal microscope allows detection from very thin optical slices in the z direction. The smaller the pinhole, the thinner the optical slice, and the better the z resolution. Hence for many biological applications, the confocal pinhole is made as small as possible to get the best overall resolution. In our experiments we want the laser beam spot in the focal plane to be the correlator so the confocal pinhole is opened to the point where it is no longer limiting the resolution. The full laser beam provides a larger correlation area and hence more points in the correlation function fit, which increases the precision of the measurement. The negative consequence of this is that we observe fewer characteristic fluctuations in an image leading to a lower accuracy. On balance, this effect is still much less than the variation in data from cell to cell in a sample. The size of the observation volume was fixed throughout the experiment. The e^{-2} radius of the laser beam was measured elsewhere [40] and was found to be around 0.4 μm (a value confirmed by the correlation function width). The laser intensity was set for minimum photobleaching by using the minimum power, LA $= 3$.

Images were collected with a time interval of 20 s between the start of consecutive images with photon counting mode set to accumulate three scans in about 5 s. A total of 15–20 images was collected for each measurement covering a period

of 200–300 s. Several measurements were performed on each sample. All the images were collected as square images with 512×512 pixels at a zoom factor of 10, corresponding to a pixel resolution of 0.032 μm in the x and y directions. We observed very little photobleaching from one image to the next. Over a total of about 20 images, the accumulated decrease in intensity was 5–10%.

2.4. Fluorescence photobleaching

Fluorescence photobleaching is based on macroscopically creating a concentration gradient in fluorescence at the membrane and observing the relaxation back to equilibrium. A fluorescent label (monoclonal antibody) is attached to the membrane receptor whose diffusion is to be studied. The labelled cells (details in Section 2.1) attached to the glass coverslips are mounted in phosphate buffer and inserted under the microscope. An argon ion laser beam is focused on a small, circular membrane area on the surface of a labelled cell to measure the fluorescence in that area. A short laser pulse (50–500 ms) destroys the fluorescence in the bleach spot. The recovery of fluorescence in the bleached area is then measured using the same attenuated laser beam. The time course of recovery of fluorescence reflects the rate of lateral mobility (diffusion coefficient) of neighbouring unbleached fluorophores into the bleached area. All the experiments were performed at room temperature (25 ± 2°C). In photobleaching experiments, the diffusion coefficient (D) and the mobile fraction (X_m) were calculated by previously published methods [6,29]. Diffusion measurements by photobleaching are over a range of about 1 μm. However a protein can be freely diffusing in a small domain but trapped by the presence of other integral proteins. These receptor proteins would then be determined to be immobile by fluorescence photobleaching.

3. Image cross-correlation function

Image cross-correlation spectroscopy is based on measurement and analysis of fluctuations in the fluorescence intensity in each pixel of images obtained as a function of time. Quantitative analysis [36] of the fluctuation is done by calculating the cross-correlation function $g_{ij}(\xi,\eta;\tau)$ for a pair of images separated in time by τ. Thus

$$g_{ij}(\xi,\eta;\tau) = \langle \delta i(x+\xi, y+\eta; t+\tau)\, \delta j(x,y;t) \rangle \tag{1}$$

where δi and δj are given by

$$\delta i(x+\xi, y+\eta; t+\tau) = \frac{i(x+\xi, y+\eta; t+\tau) - \langle i(x,y;t+\tau) \rangle}{\langle i(x,y;t+\tau) \rangle} \tag{2}$$

$$\delta j(x,y;t) = \frac{j(x,y;t) - \langle j(x,y;t) \rangle}{\langle j(x,y;t) \rangle} \tag{3}$$

and $j(x,y;t)$ is the intensity at a particular location in one image collected at time t and $i(x,y;t+\tau)$ is the intensity at the same location in another image collected at a later time, $t+\tau$. The angular brackets denote averages over the entire image. For diffusion in a Gaussian illumination volume, we expect from the original fluorescence

Table 1
Comparison of diffusion and cluster densities of transferrin receptors on 3T3 mouse fibroblasts and human HEp2 cells. Error represents the standard error of the mean. N is the number of measurements

	$\langle i \rangle$	CD μm^{-2}	N	D_{ICCS} 10^{-12} cm^2/s	N	D_{FPR} 10^{-9} cm^2/s	X_m	N
3T3	1.0 ± 0.4	21 ± 4	110	1.9 ± 1.0	73	6.8 ± 2.1	0.6	49
HEp2	6.5 ± 0.6	17 ± 3	92	1.5 ± 1.2	56	2.9 ± 1.3	0.5	41

correlation spectroscopy (FCS) theory [3,4,31] that:

$$g_{ij}(0,0;\tau) = \frac{g_{ij}(0,0;0)}{1+\frac{\tau}{\tau_d}} + C. \quad (4)$$

where τ_d is the characteristic decay time related to a diffusion coefficient, D, by $\tau_d = \omega^2/4D$ and ω is the $1/e^2$ radius of the focused laser beam. C is a constant added to allow for incomplete decay of correlations at longer time due to immobile fluorescent molecules and limited data records. The values of $g_{ij}(0,0;0)$, C and τ_d are determined by fitting the experimental data to Eq. (4). The $g_{ij}(0,0;0)$ value is the inverse of the average occupation number $\overline{N}$ of the fluorescent entities (receptor clusters) present in the observation area of the laser beam i.e. $g_{ij}(0,0;0) = 1/\overline{N}$. From the amplitude of the cross-correlation function, $g_{ij}(0,0;0)$, we can then calculate the cluster density (CD) which is defined as the average number of clusters per square micrometre of membrane:

$$\mathrm{CD} = \frac{1}{g_{ij}(0,0;0)\pi\omega^2} \quad (5)$$

4. Results

4.1. Distribution of transferrin receptors on mouse 3T3 fibroblasts and human HEp2 cells

An example of a confocal image of section of 3T3 fibroblast exposed to transferrin receptor specific antibody is shown in Fig. 1A. Clearly, we can see that there are a large number of distinct regions on the cell surface that are labelled with the fluorescent antibody. The fluorescent intensity profile of each small region represents the intensity profile of the excitation laser. A two-dimensional autocorrelation analysis of the single image [40] was performed as shown in Fig. 1B. The two dimensional fit gives values for $g_{ij}(0,0,0)$, ω and the average intensity in the image, $\langle i \rangle$. Estimates of contributions from correlated noise

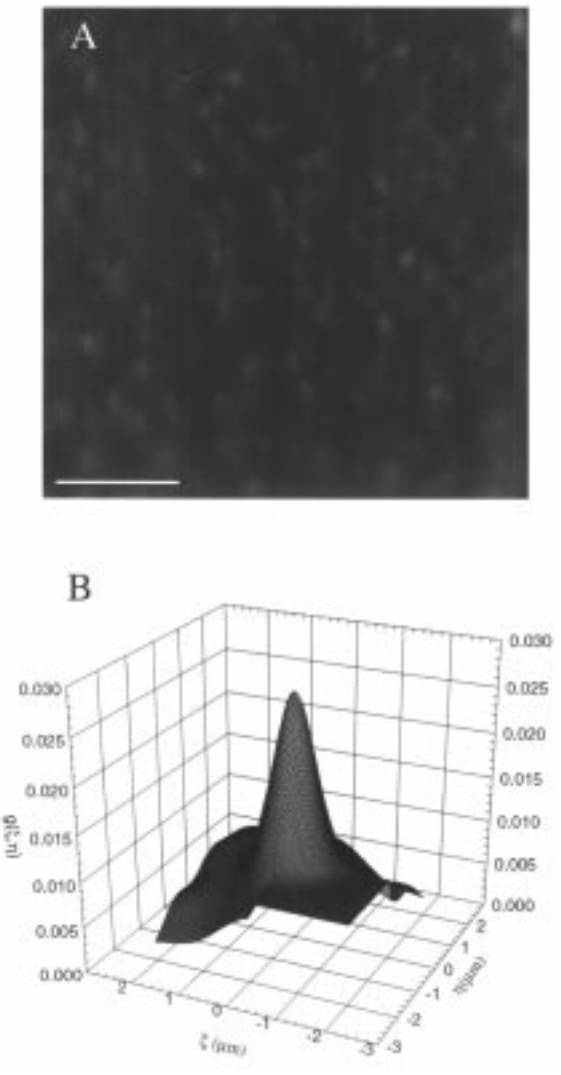

Fig. 1. (A) A zoom 10 confocal laser scanning microscope image (512 × 512 pixels) from the mouse 3T3 fibroblast. The fluorescent spots in the image represent the spatial locations of labelled transferrin receptors with the cell membrane area sampled. The image was collected with FITC optics in photon counting mode and is an accumulation of 25 scans. The image has dimensions of 16.3 μm × 16.3 μm. The scale bar represents 4.1 μm. (B) A plot of the discrete estimate of the normalized fluorescence intensity fluctuation autocorrelation function (cross-correlation of image depicted in Fig. 1A by itself) as a function of spatial lag in the two independent image directions. The Gaussian function of best fit to the auto-correlation data is plotted in the near quadrant, while the other three quadrants contain the discrete correlation function data.

sources were obtained by imaging many samples which were controls for autofluorescence and non-specific labelling. The intensity arising from these controls was subtracted from the original intensity to get the intensity due to the true signal (i.e. due to specifically bound fluorophores). The image correlation spectroscopy [40] was applied to 90–110 cells to get good information about the number density of transferrin receptor clusters (fluorescent entities) on the surface of 3T3 and HEp2 cells, respectively. Table 1 shows the values of $g_{ij}(0,0,0)$ and the cluster density (CD). In the case of HEp2 cells, the clusters are larger and brighter but fewer in number as compared to 3T3 fibroblasts. Since all the samples were prepared at 4°C (on ice), we assume that there was no antibody-induced clustering. Since lateral diffusion is very slow at 4°C [18] there are no obvious differences between distributions of receptors obtained on fixed cells and on live cells at 4°C.

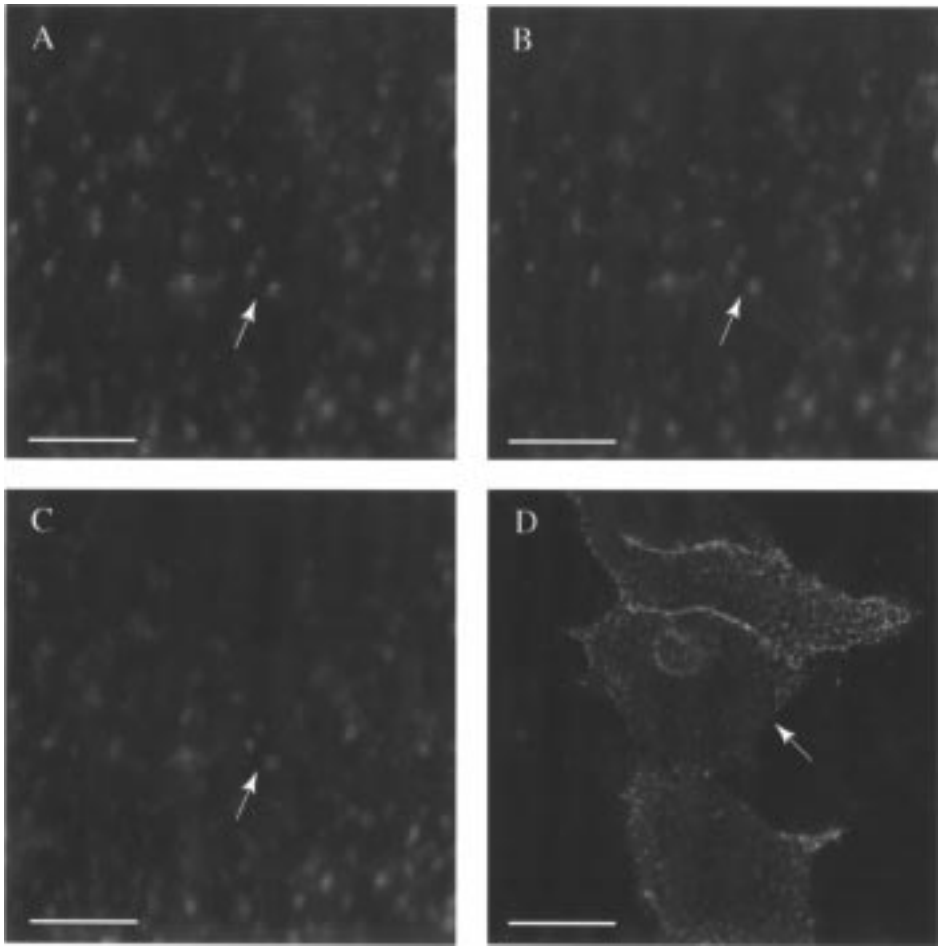

Fig. 2. Zoom 10 confocal images of the sections of the mouse 3T3 fibroblast collected at (A) 0 s; (B) 25 s; (C) 175 s with FITC optics in photon counting mode and is an accumulation of three scans. Arrows in these images show the position of a particular receptor cluster at the specified times. The image has dimensions of 16.3 μm $\times$ 16.3 μm. (D) Confocal image showing overview of 3T3 fibroblast. The faint region (bleach box) in the central cell shows the membrane area from which zoom 10 images were sampled at specified times for subsequent ICCS analysis. This box has been created after 45 scans of the region during the collection of one set of data, i.e. 15 images collected with a time interval of 20 s in between the images with three scans for each collection. The scale bar represents 4.1 μm.

4.2. Diffusion measurements of transferrin receptor clusters on mouse 3T3 fibroblasts and human HEp2 cells using ICCS at room temperature (25 ± 2°C)

We performed experiments on the surface of live cells to get information about the dynamics of receptors on the surface of the cells. For this we labelled the cells on ice with FITC conjugated monoclonal antibody specific for the transferrin receptors. Fig. 2 shows three images (A, B, C) from a series of 15 images collected on the same area of a cell (D) at 20-s intervals. The arrows in images A to C show the positions of a set of receptor clusters. Over this time scale, the movement of the clusters is less than or comparable to the dimension of the laser beam (as indicated by the size of each spot). A total of 30–40 sets of 15 images were collected to measure the amplitude

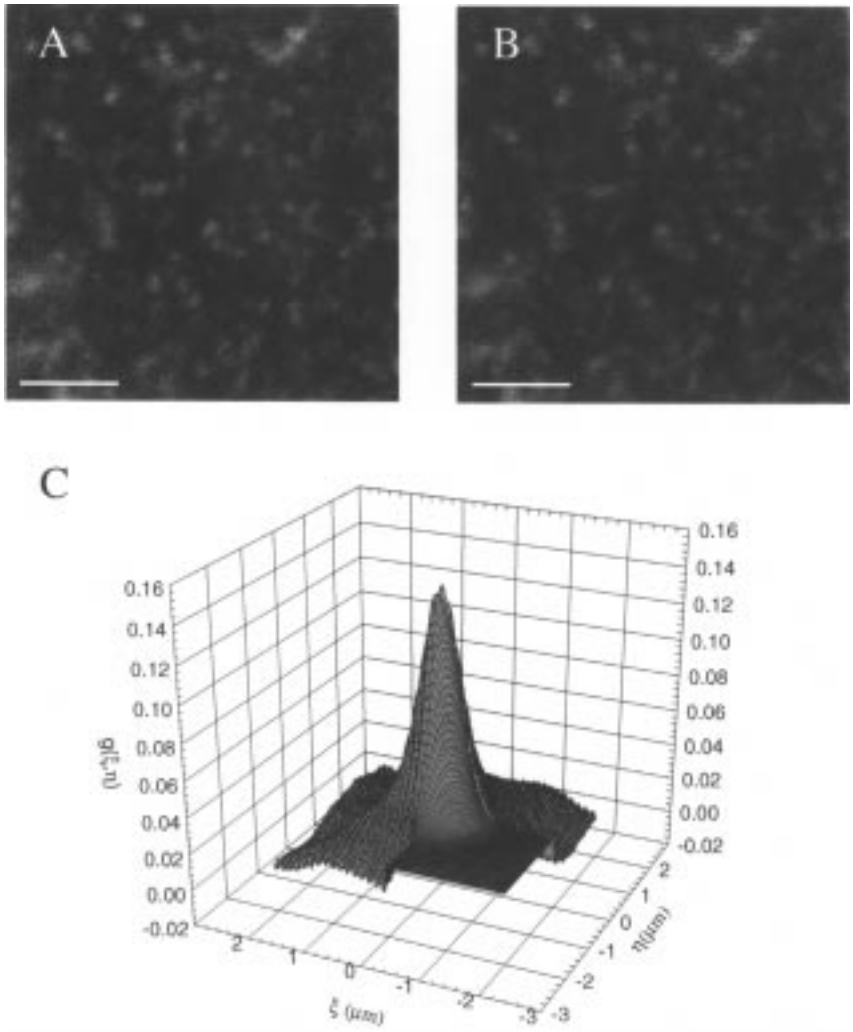

Fig. 3. Zoom 10 confocal images of the section of human HEp2 cell collected at (A) 0 s; (B) 25 s with FITC optics in photon counting mode and is an accumulation of three scans. (C) Plot of the cross-correlation function between the two images A and B, as a function of spatial lag in the two independent image directions. The Gaussian function of best fit to the auto-correlation data is plotted in the near quadrant, while the other three quadrants contain the discrete correlation function data. The scale bar represents 4.1 μm.

of the cross-correlation function as a function of time ($g_{ij}(0,0;\tau)$).

Fig. 3C shows an example of the cross-correlation function obtained from the images in Fig. 3A and B, which were collected from the surface of HEp2 cells at two different times. The Gaussian function of best fit to the cross-correlation function is plotted in the near quadrant. The other three quadrants contain the discrete cross-correlation function data. The value of the amplitude, $g_{ij}(0,0;\tau)$, is determined from this cross-correlation function by extrapolation of the fit to the origin. Fig. 4 shows an example of the variation of the amplitude of the cross-correlation function as a function of delay time between the images, τ. The solid line indicates the best fit to Eq. (4). From the fitting parameters, both the number density, $N = 1/g_{ij}(0,0;0)$ and diffusion coefficient, $D = \omega^2/4\tau_d$ can be calculated. This experiment was performed on several samples and several measurements (3–5) were made on each sample. We did this experiment on two different cell types, mouse 3T3 fibroblasts and human HEp2 cells. The results are tabulated in Table 1. The value of diffusion coefficients are small and are almost the same for both cell types.

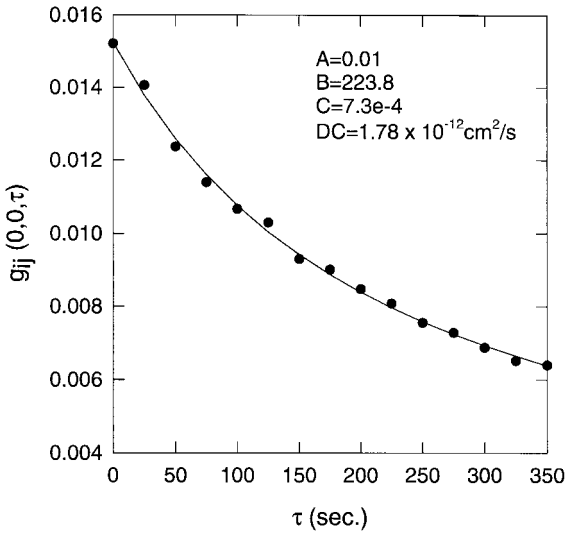

Fig. 4. Plot of the amplitude of the cross-correlation function, $g_{ij}(0,0,\tau)$, as a function of delay time, τ. The smooth curve is the best fit to the Eq. (4). For this curve A = 0.01, B = 223.8, C = 7.4e − 4 and diffusion coefficient, D, is calculated to be 1.78×10^{-12} cm^2/s.

4.3. Fluorescence photobleaching recovery

Table 1 also summarises the results of the diffusion coefficient (D) and the mobile fraction (X_m) of transferrin receptors on 3T3 and HEp2 cells using standard photobleaching techniques (Fig. 5).

5. Discussion

Movements of transferrin receptor clusters in the cell membrane of cultured 3T3 fibroblasts and HEp2 cells were investigated using the new technique of image cross correlation spectroscopy (ICCS) [36]. The lateral mobility of membrane components has been extensively probed by fluorescence photobleaching [5,6,27,29,31] and more recently by single particle tracking (SPT) [19,20,25,26,28,34,35]. It is generally observed that membrane proteins diffuse laterally in the membrane plane unless constrained by interactions with immobile or slowly moving components. Fluorescence photobleaching measurements of lateral diffusion normally assumes that receptors are either diffusing randomly or are immobile. From SPT studies of diffusion of transferrin receptors in the plasma membrane [21,25,26,41] it was found that most of the movement was of confined diffusion type within domains. Movement within domains is random with a diffusion coefficient of $\sim 10^{-9}$ cm^2/s, which is consistent with that expected from free Brownian diffusion of proteins in the plasma membrane and with our photobleaching results. There is another population of receptors which exhibit slower diffusion ($\sim < 10^{-11}$ cm^2/s), due to interactions with the cytoskeleton, cytoplasmic constituents, entrapment in flat clatherin lattices, or with intramembranous proteins and lipids. Previous work using video enhanced contrast optical microscopy [14,25] reveals the presence of two populations of transferrin receptors in the plasma membrane in terms of their responses to lateral dragging forces exerted by laser tweezers at 100 mW (mobile and immobile population). Slow diffusion is considered immobile in photobleaching experiments.

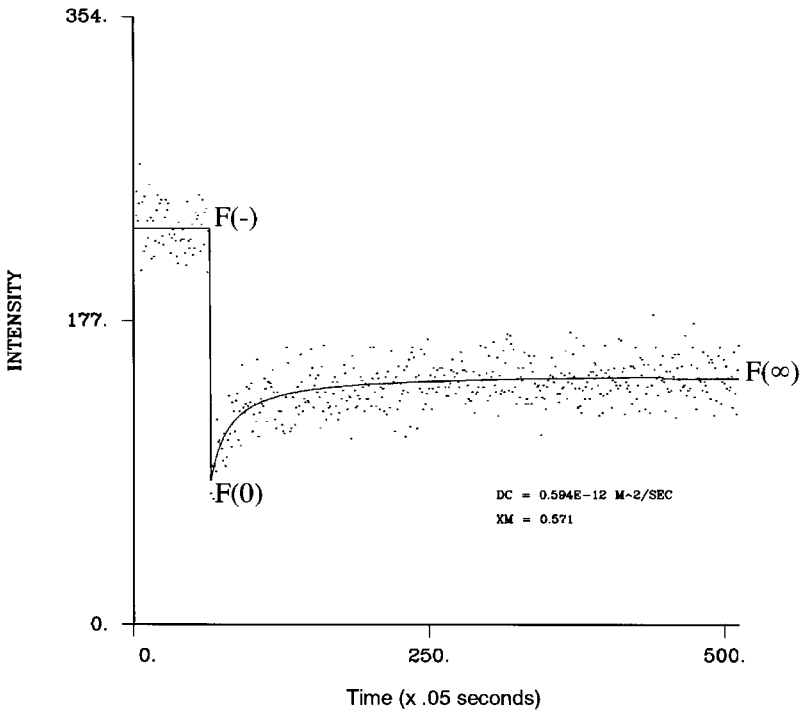

Fig. 5. Sample FPR curve obtained for FITC-transferrin-labelled receptors on mouse 3T3 fibroblast illustrating the steps in an FPR experiment. Here F(−) represents the pre-experiment fluorescence level, F(0) is the fluorescence level immediately after photobleaching and F(∞) is the recovered fluorescence intensity of the bleach spot through the process of lateral diffusion of the FITC-labelled-transferrin receptors. Here X_m is the mobile fraction which is defined by $X_m = \{F(\infty) - F(0)\}/\{F(-) - F(0)\}$ and DC is the diffusion coefficient.

All the above mentioned methods measure diffusion coefficient of a single receptor monomer. In contrast the low values of the measured diffusion coefficient (D) suggests that image cross-correlation spectroscopy (ICCS) measures the mobility (diffusion) of clusters (aggregates) of receptors. Therefore direct comparison of photobleaching data with ICCS data is inappropriate because fluorescence photobleaching method records the fast exchange diffusion for one component (receptor monomer) and the slow diffusion is considered immobile in these results. In ICCS, the highly mobile receptors move beyond the correlation distance between images so they do not contribute to the correlation function and are left undetected. These highly mobile receptors will contribute to the average intensity, $\langle i \rangle$, and may lead to underestimates of the $g(0,0;0)$ values.

Fig. 6 shows a schematic representation of the diffusion coefficient as measured by photobleaching method (D_{FPR}) vs. the diffusion coefficient measured by image cross-correlation spectroscopy (ICCS) technique (D_{ICCS}). The circular boundary represents the laser beam area. Here we see that D_{ICCS} measures the mobility of the whole receptor cluster (grey dots enclosed in dashed boundary moving to black dots enclosed in the solid boundary) which is slow. Whereas D_{FPR} measures the mobility of a single receptor monomer, diffusing from one cluster to another cluster or from one cluster to outside the beam area which is considerably faster.

Like the photobleaching method, the present approach samples the entire population as a function of time, but the cross-correlation analysis yields the ensemble averaged diffusion coefficients only giving information on the behaviour of a large group of molecules. The loss of detailed

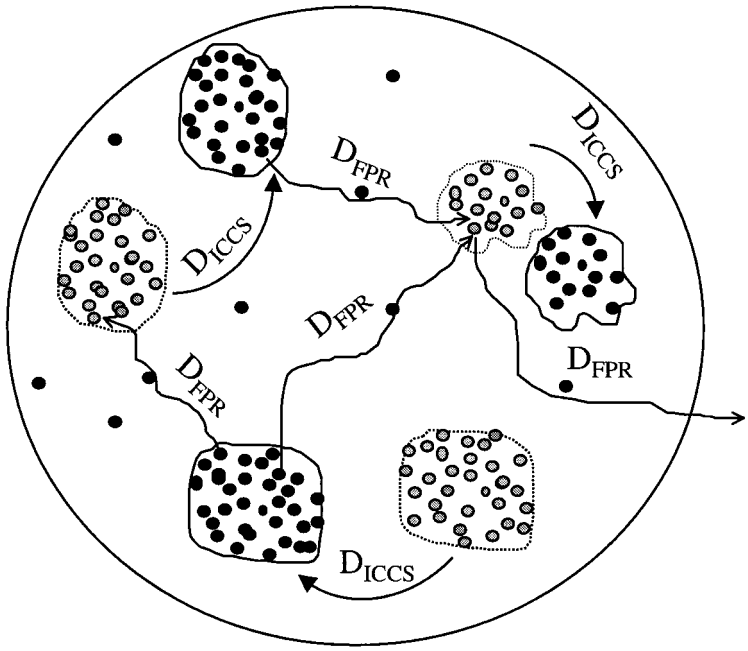

Fig. 6. Schematic representation of the difference in the diffusion coefficient as measured by photobleaching method (D_{FPR}) vs. ICCS method (D_{ICCS}). Here the circular boundary represents the laser beam area focusing the receptor clusters. Each dot (grey or black) represents a receptor monomer and the boundaries (dashed or solid) enclosing the dots represent the receptor clusters (aggregates). Dashed boundaries enclosing grey dots represent receptor clusters at any one time and the solid boundary enclosing black dots represents receptor clusters at a later time.

distribution of diffusion coefficient is compensated for, in part, by the ease and speed of analysis. The details of receptor movement have important implications for any biological process that involves dynamic interactions in the cell surface membrane. Further development of the imaging techniques (ICCS) described here promises to make a significant contribution to the quantitative understanding of slow processes. In cases where the variation in diffusion behaviour varies from sample to sample, e.g. cell to cell in a biological study, ICCS may provide a more convenient approach to measuring the slow dynamic processes as long as information about the average property is sufficient.

In addition to the single channel method of ICCS we have discussed, it is also possible to use a second channel to obtain a second fluctuation signal [36]. Using the cross-correlation function from the two channels, as a function of time, will ultimately permit measurement of kinetics of association or dissociation of two receptor types in a cell membrane.

Acknowledgements

This work has been supported by the National Sciences and Engineering Research Council of Canada NSERC (OGP 3272). Also we thank Paul St-Pierre for helping us with some of the parallel programs on the massively parallel computer (MasPar MP-2) and Cuihua Liu to help us start with the photobleaching experiment.

References

[1] S.J. Singer, G.L. Nicolson, Science 175 (1972) 721.
[2] J. Schlessinger, Trends Biochem. Sci. 5 (1980) 210.
[3] E.L. Elson, D. Magde, Biopolymers 13 (1974) 1.
[4] D. Magde, E.L. Elson, W.W. Webb, Biopolymers 13 (1974) 29.
[5] R. Peters, J. Peters, K.H. Tews, W. Bàhr, Biochim. Biophys. Acta 367 (1974) 282.

[6] D. Axelrod, D.E. Koppel, J. Schlessinger, E.L. Elson, W.W. Webb, Biophys. J. 16 (1976) 1055.
[7] B.A. Smith, W.R. Clark, H.M. McConnell, Proc. Natl. Acad. Sci. USA 76 (1979) 5641.
[8] W.W. Webb, L.S. Barak, D.W. Tank, E.-S. Wu, Biochem. Soc. Symp. 46 (1981) 191.
[9] L.S. Barak, W.W. Webb, J. Cell Biol. 95 (1982) 846.
[10] N.O. Petersen, Can. J. Biochem. 62 (1984) 1158.
[11] H.G. Kapitza, G. McGregor, K.A. Jacobson, Proc. Natl. Acad. Sci. USA 82 (1985) 4122.
[12] N.O. Petersen, Biophys. J. 49 (1986) 809.
[13] H.G. Kapitza, K. Jacobson, in: C.J. Ragan, R.J. Cherry (Eds.), Techniques for the Analysis of Membrane Proteins, Chapman and Hall, London, 1986, pp. 345–375.
[14] H. Geerts, M. De Brabander, R. Nuydens, et al., Biophys. J. 52 (1987) 775.
[15] I.E.G. Morrison, C.M. Anderson, G.N. Georgiou, R.J. Cherry, Biochem. Soc. Trans. 18 (1990) 938.
[16] M. De Brabander, R. Huydens, A. Ishihara, B. Holifield, K. Jacobson, H. Geerts, J. Cell Biol. 112 (1991) 111.
[17] G.M. Lee, A. Ishihara, K.A. Jacobson, Proc. Natl. Acad. Sci. 88 (1991) 6274.
[18] C.M. Anderson, G.N. Georgiou, I.E.G. Morrison, G.V.W. Stevenson, R.J. Cherry, J. Cell Sci. 101 (1992) 415.
[19] A. Kusumi, Y. Sako, M. Yamamoto, Biophys. J. 65 (1993) 2021.
[20] R.N. Ghosh, W.W. Webb, Biophys. J. 66 (1994) 1301.
[21] Y. Sako, A. Kusumi, J. Cell Biol. 125 (1994) 1251.
[22] I.E.G. Morrison, C.M. Anderson, G.N. Georgiou, G.V.W. Stevenson, R.J. Cherry, Biophys. J. 67 (1994) 1280.
[23] U. Kubitscheck, P. Wedekind, R. Peters, Biophys. J. 67 (1994) 948.
[24] D.E. Koppel, F. Morgan, A.E. Cowan, J.H. Carson, Biophys. J. 66 (1994) 502.
[25] Y. Sako, A. Kusumi, J. Cell Biol. 129 (1995) 1559.
[26] R.N. Ghosh, F.R. Maxfield, J. Cell Biol. 128 (1995) 549.
[27] T.J. Feder, I. Brust-Mascher, J.P. Slattery, B. Baird, W.W. Webb, Biophys. J. 70 (1996) 2767.
[28] K.M. Wilson, I.E.G. Morrison, P.R. Smith, N. Fernandez, R.J. Cherry, J. Cell Sci. 109 (1996) 2101.
[29] K. Jacobson, Z. Derzko, E.-S. Wu, Y. Hou, G. Poste, J. Supramol. Struct. 5 (1976) 565.
[30] B.G. Barisas, M.D. Leuther, Biophys. Chem. 10 (1979) 221.
[31] N.O. Petersen, E.L. Elson, Methods Enzymol. 130 (1986) 454.
[32] T. Jovin, W.L.C. Vaz, Methods Enzymol. 172 (1989) 471.
[33] R. Peters, in: R.J. Cherry (Ed.), New Techniques of Optical Microscopy and Microspectroscopy, The Macmillan Press, Basingstoke, 1991, pp. 199–228.
[34] F. Zhang, G.M. Lee, K. Jacobson, BioEssays 15 (1993) 579.
[35] R. Simson, E.D. Sheets, K. Jacobson, Biophys. J. 69 (1995) 989.
[36] M. Srivastava, N.O. Petersen, Methods Cell Sci. 18 (1996) 47.
[37] P. St-Pierre, Submicron Correlations of Receptor-Positions on Cell Surfaces, Ph.D. Thesis, 1992, p. 82.
[38] M.C. Willingham, F.R. Maxfield, I.H. Pastan, J. Cell Biol. 82 (1979) 614.
[39] J. Boonstra, P. Van Maurik, L.H.K. Defize, S.W. de Latt, J.L.M. Leunissen, A.J. Verkley, Euro. J. Cell Biol. 36 (1985) 209.
[40] N.O. Petersen, P.A. Hoddelius, P.W. Wiseman, O. Seger, K.-E. Magnusson, Biophys. J. 65 (1993) 1135.
[41] R.N. Ghosh, D.L. Gelman, F.R. Maxfield, J. Cell Sci. 107 (1994) 2177.